Available online at www.sciencedirect.com
ScienceDirect
Catalysis Today 131 (2008) 140–145
CATALYSIS TODAY
www.elsevier.com/locate/cattod

Dehydrogenation of ethylbenzene with carbon dioxide over MgO-modified Al_2O_3-supported V–Sb oxide catalysts

Do-Young Hong [a], Vladislav P. Vislovskiy [a], Young Kyu Hwang [a], Sung Hwa Jhung [b], Jong-San Chang [a,*]

[a] *Catalysis Center for Molecular Engineering, Korea Research Institute of Chemical Technology (KRICT), P.O. Box 107, Yusung, Taejon 305-600, Republic of Korea*
[b] *Department of Chemistry, College of Natural Sciences, Kyungpook National University, Daegu 702-701, Republic of Korea*

Available online 26 November 2007

Abstract

Alumina-supported $V_{0.43}Sb_{0.57}$ oxide (VSb/Al) and MgO-modified alumina-supported $V_{0.43}Sb_{0.57}$ oxide catalysts (VSb/Mg_nAl with Mg/Al atomic ratio, $n = 0.1$, 0.3 or 0.5) have been tested for the dehydrogenation of ethylbenzene with carbon dioxide as an oxidant. Their catalytic behaviors were interpreted by results of several catalyst characterization methods. The decrease in the surface acidity of the VSb/Mg_nAl catalysts due to modification of alumina with MgO favors the prolonged time-on-stream activities. However, the addition of relatively large amounts of MgO ($n = 0.3$ or 0.5) causes substantial decrease in their surface areas, reducibility of active vanadium oxide component and, consequently, ethylbenzene conversion. These negative factors did not become apparent for the most efficient VSb/$Mg_{0.1}$Al system demonstrating high and stable catalytic activity.

Keywords: Ethylbenzene; Dehydrogenation; Styrene; Carbon dioxide; Supported V–Sb oxide catalysts; MgO-modified alumina support

1. Introduction

Styrene, one of the most important basic monomers in the chemical industry, is produced commercially by the large-scale ethylbenzene dehydrogenation (EBDH) processes with steam. However, the steam-based EBDH process has inherent drawbacks: thermodynamic limitations for EB-conversion, high-energy requirements due to endothermic reaction and lose of latent heat of steam during its condensation and subsequent separation [1,2]. The use of traditional oxidant – oxygen – overcomes the thermodynamic limitations and helps to operate the reaction at lower temperatures due to its exothermic nature. However, O_2-EBDH process suffers from a significant loss of styrene selectivity due to formation of total oxidation products and has a number of safety issues [1]. Another oxidant – carbon dioxide – looks very promising for the development of safer, more economical and environmentally friendly CO_2-EBDH process that utilizes CO_2, a greenhouse gas, instead of its release to atmosphere [2,3].

Several catalyst systems containing metal oxides of Fe, V and Cr were found to be active and selective in the ethylbenzene dehydrogenation with carbon dioxide [3–15]. However, catalytic activity of these catalysts decreased during a few hours on stream. Our highly active and very selective $V_{0.43}Sb_{0.57}O_x/Al_2O_3$ catalyst for the CO_2-EBDH is relatively more stable than other reported systems, but the decrease of styrene yield (from 76% after 1 h to 70% after 7 h) is also significant [12,13]. Therefore, a main objective of this work is to improve catalyst stability of the alumina-supported $V_{0.43}Sb_{0.57}O_x$ system.

It has been reported that catalytic activity of $V_{0.43}Sb_{0.57}O_x/Al_2O_3$ in the CO_2-EBDH decreases mainly due to formation of coke [12,13]. The coke precursors are formed in the EBDH by the oligomerization of styrene [1]. Its fast desorption from a catalyst surface prevents this reaction and therefore could minimize the coke accumulation. More rapid desorption of olefin as a base is expected from a catalyst surface with poor acidity [16,17] that can be controlled by the introduction of alkali or alkaline earth oxides such as magnesia [17,18].

* Corresponding author. Tel.: +82 42 860 7673; fax: +82 42 860 7676.
E-mail address: jschang@krict.re.kr (J.-S. Chang).

0920-5861/$ – see front matter © 2007 Published by Elsevier B.V.
doi:10.1016/j.cattod.2007.10.020

Alumina has moderate Lewis acid sites on the surface, whereas $MgAl_2O_4$ possesses acid–base sites with low strength as compared with MgO and Al_2O_3 [19]. In the propane oxidative dehydrogenation, VO_x-loaded catalysts on MgO-modified alumina exhibited a decrease in the adsorption of olefin compared to the catalyst on unmodified support [18]. Based on such considerations, an attempt in this work has been made to improve the stability of the $V_{0.43}Sb_{0.57}O_x/Al_2O_3$ in the CO_2-EBDH by introduction of MgO to alumina support. The relationships between catalytic activities and structural features of catalysts were studied by several characterization methods.

2. Experimental

2.1. Catalyst preparation

MgO-modified alumina (Mg_nAl; n is atomic mole ratio, Mg/Al = 0.1, 0.3 or 0.5) supports were obtained by impregnation for 2 h at room temperature of activated alumina (Aldrich, S_{BET} = 121 m^2/g) with aqueous solutions containing a certain amount of $Mg(NO_3)_2{\cdot}6H_2O$. The Mg_nAl supports were calcined at 670 °C for 4 h in air. Alumina (Al)- or Mg_nAl-supported vanadium–antimony oxide catalysts were prepared by impregnation for 2 h at room temperature with the solutions of NH_4VO_3 and $SbCl_3$ along with tartaric acid. The catalysts were dried at 120 °C and then calcined at 650 °C for 4 h in air. The loading of the supported $V_{0.43}Sb_{0.57}O_x$ component (20 wt.%) was the same for all samples.

2.2. Catalyst characterization

The fresh catalysts were characterized by BET-specific surface area (S_{BET}), X-ray diffraction (XRD), thermal gravimetric analysis (TGA), hydrogen temperature-programmed reduction (H_2-TPR), ammonia temperature-programmed desorption (NH_3-TPD) and UV–vis diffuse reflectance (DR) spectrometric methods. S_{BET} data were measured by nitrogen adsorption isotherms at liquid nitrogen temperature with Tristar 3000 model from Micrometrics. Samples were previously degassed at 300 °C for 2 h. Surface area was obtained by BET linearization in the pressure range 0.05–0.2p/p_0. The average pore sizes were calculated by the BJH method. XRD patterns were recorded with a Miniflex diffractometer from Rigaku using monochromatic Cu Kα radiation. TGA was carried out with the apparatus DMA from TA Instruments under air within the temperature range 25–1000 °C at a heating rate 10 °C/min. H_2-TPR experiments were carried out with a Micrometrics model Pulse Chemisorb 2705 system equipped with a thermal conductivity detector (TCD) for monitoring of the H_2 consumption. The samples were pretreated in a flow of 10% O_2/N_2 at 600 °C for 2 h. TPR experiments were performed in the temperature range of 100–800 °C in a flow of 5% H_2/N_2 (15 ml/min). The rate of heating was 10 °C/min. NH_3-TPD experiments were carried out in the same instrument as used for H_2-TPR. The catalysts were pretreated at 600 °C for 1 h in a flow of 10% O_2/N_2 (15 ml/min) followed by purging with nitrogen and then cooling to 100 °C. Then adsorption of ammonia was performed at 100 °C for 1 h to avoid adsorption of water on acid sites of the catalysts. The physisorbed ammonia was removed in a flow of dry nitrogen at 100 °C for 30 min. The TPD of the chemisorbed was carried out between 100 and 600 °C with a heating rate 10 °C/min in a flow of nitrogen. UV–vis DR spectroscopic measurements were recorded with a UV-250 1PC spectrophotometer from Shimadzu. The spectra were recorded in the range of 200–800 nm referenced to $BaSO_4$. The catalyst samples were loaded into a cell and, before the measurement, samples were subjected to two types of pretreatments: under a vacuum at 300 °C for 1 h and in O_2-flow at 600 °C for 1 h.

2.3. Catalytic measurements

The catalytic tests were carried out in an isothermal fixed bed flow reactor (continuous micro-activity test unit, Zeton, MAT 2000) using 1 g of catalyst at 595 °C under atmospheric pressure. The ethylbenzene feed rate was 8.2 mmol/h (weight hourly space velocity, WHSV = 1 h^{-1}), molar ratio CO_2/EB = 5, total flow rate of the gas mixture was 45 ml/min. Nitrogen was used as inert diluent component as well as the internal standard for gas analysis. Gas components of the reaction mixture (H_2, N_2, CO, CH_4, CO_2) were analyzed by TCD of the on-line gas chromatograph (Donam Instrument DS6200). Liquid products (benzene, toluene, ethylbenzene, styrene) were analyzed by FID. The ethylbenzene conversion, X_{EB}, styrene yield, Y_{ST} and styrene selectivity, S_{ST}, are expressed as mol.% on a carbon atom basis.

3. Results

Table 1 and Fig. 1 present the catalytic properties of the VSb/Al and VSb/Mg_nAl oxide systems in the CO_2-EBDH at 595 °C. For all catalysts, styrene was identified as a main product together with hydrogen, carbon monoxide and water. Benzene and toluene (along with methane) were obtained as cracked by-products in much lower amounts, i.e. all these catalysts demonstrated similar high selectivity to styrene, S_{ST} = 95–97%. From the major reaction products, it can be interpreted that non-oxidative ($PhCH_2CH_3 \leftrightarrow PhCH=CH_2 + H_2$) and oxidative ($PhCH_2CH_3 + CO_2 \rightarrow PhCH=CH_2 + CO + H_2O$) pathways are competed in the EBDH with CO_2. It cannot be excluded also substantial contribution from the reverse water-gas shift reaction ($CO_2 + H_2 \leftrightarrow CO + H_2O$), in which CO_2 reacts (also as an oxidant) with hydrogen dissociated from EB under the non-oxidative EBDH reaction.

After 1 h on stream, the VSb/Al and VSb/$Mg_{0.1}Al$ catalysts showed identical ethylbenzene conversions and styrene yields ($Y_{ST} \sim 75\%$) (Fig. 1 and Table 1). The VSb/$Mg_{0.3}Al$ and VSb/$Mg_{0.5}Al$ catalysts displayed lower ethylbenzene conversion and styrene yield (~47% and 30%, respectively) which result due to substantially decrease in specific surface areas. VSb/$Mg_{0.1}Al$ system is found to be little more active catalyst due to its higher areal rate (moles of produced styrene per minute per surface area), 1.6 μmol/min m^2 against 1.2 μmol/min m^2 for the VSb/Al. The areal rate (1.1–1.4 μmol/min m^2) obtained for the

Table 1
Catalytic behavior of VSb/Al and VSb/Mg_nAl oxide systems in the CO_2-EBDH and some physicochemical properties of the catalysts and supports

Catalyst or support	S_{BET} (m^2/g)	Pore volume (ml/g)	Average pore size (nm)	Phase composition (XRD)	X_{EB}[a] (%)	Areal rate[b] (μmol/min m^2	Y_{ST}[a] (%)	Coke amount[c] (wt.%)
Al	121	0.28	7.9	Al_2O_3 (almost amorphous)	–	–	–	–
VSb/Al	87	0.23	5.2	Al_2O_3, $V_{1.1}Sb_{0.9}O_4$	78	1.2	75	13.1
$Mg_{0.1}$Al	116	0.26	7.9	$MgAl_6O_{10}$	–	–	–	–
VSb/$Mg_{0.1}$Al	67	0.20	7.2	$MgAl_6O_{10}$, $V_{1.1}Sb_{0.9}O_4$	77	1.6	75	4.4
$Mg_{0.3}$Al	68	0.20	10.2	$MgAl_2O_4$, MgO (weak)	–	–	–	–
VSb/$Mg_{0.3}$Al	48	0.14	8.8	$MgAl_2O_4$,$V_{1.1}Sb_{0.9}O_4$ (weak)	49	1.4	47	4.8
$Mg_{0.5}$Al	59	0.14	10.3	$MgAl_2O_4$, MgO (strong)	–	–	–	–
VSb/$Mg_{0.5}$Al	38	0.13	9.7	$MgAl_2O_4$, MgO (traces)	31	1.1	30	6.0

[a] After 1 h reaction at 595 °C, molar ratio CO_2/EB = 5 and WHSV = 1 h^{-1}.
[b] Moles of produced styrene per minute per surface area.
[c] In the used catalysts after 12 h on stream.

VSb/$Mg_{0.3}$Al and VSb/$Mg_{0.5}$Al catalysts are also very close to that for the VSb/Al catalyst. All Mg-containing catalysts exhibited much more stable activities compared to the VSb/Al (Fig. 1), evidently, due to suppression of coking. The content of carbon accumulated after 12 h on stream (measured by TGA) was substantially lower on the Mg-modified catalysts (4.4–6.0 wt.%) as compared with VSb/Al (13.1 wt.%) (Table 1).

For all supports and catalysts, N_2-adsorption isotherms obtained were typical for the mesoporous solids. As shown in Fig. 2 and Table 1, the pores of the samples almost do not contain micropores (<2 nm). BET surface area and average pore size for Al and $Mg_{0.1}$Al supports are comparable. However, with increase of the MgO-content in the Mg_nAl supports (n = 0.3 or 0.5), substantial drop of S_{BET} values from ~120 to 68–59 m^2/g parallel to the increase of the average pore size from ~7.9 to ~10.3 nm is observed. The loading of the V–Sb–O component on all these supports results in essential decrease in the catalysts BET surface area, total pore volume and average pore size. The decrease in pore sizes for Mg_nAl supports, however, is smaller than alumina support. Nevertheless, pores sizes of all catalysts are still in a mesoporous scale demonstrating that there is no diffusion limitations during adsorption and catalysis because the molecular dimension of ethylbenzene is much smaller (0.61 nm [20]) than the catalyst pore sizes (5.2–9.7 nm).

The results of XRD investigation of phase compositions of the supports and catalysts are the followings (Table 1; see also [14]). Alumina is almost amorphous in XRD. $Mg_{0.1}$Al support does not contain a free crystalline phase of MgO, it is

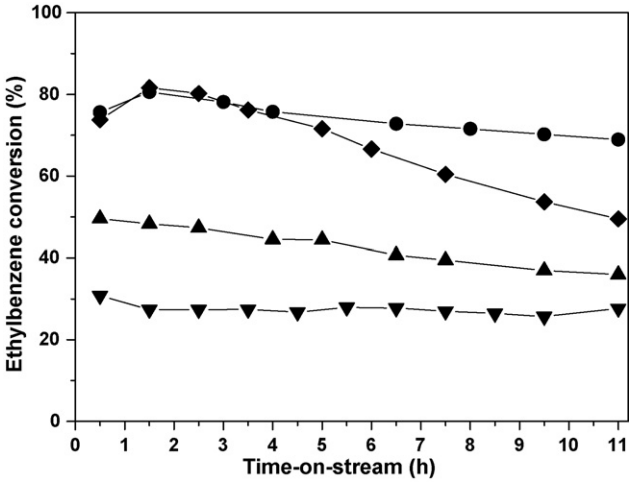

Fig. 1. Catalytic dehydrogenation of ethylbenzene with carbon dioxide at 595 °C over VSb/Al (◆) and VSb/Mg_nAl with n = 0.1 (●), n = 0.3 (▲) and n = 0.5 (▼).

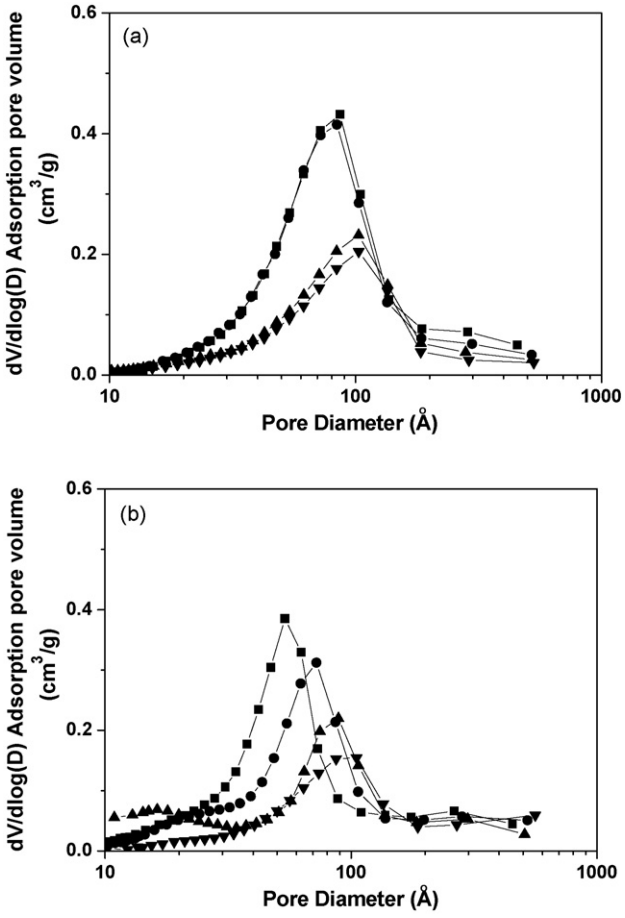

Fig. 2. Pore size distribution of (a) Al and Mg_nAl supports and (b) VSb/Al and VSb/Mg_nAl catalysts with n = 0 (■), n = 0.1, (●), n = 0.3 (▲) and n = 0.5 (▼).

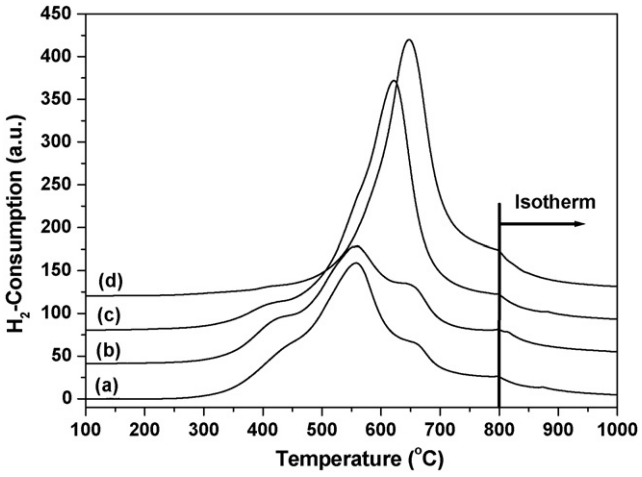

Fig. 3. H_2-TPR profiles of (a) VSb/Al, (b) VSb/$Mg_{0.1}$Al, (c) VSb/$Mg_{0.3}$Al and (d) VSb/$Mg_{0.5}$Al catalysts.

completely incorporated into a spinel-like binary oxide phase, $MgAl_6O_{10}$, whereas a crystalline MgO is clearly observed in the $Mg_{0.3}$Al and especially in the $Mg_{0.5}$Al support whose major phase is spinel-like binary oxide $MgAl_2O_4$. Traces of free MgO-phase are also seen in the VSb/$Mg_{0.5}$Al catalyst.

The vanadium–antimony mixed oxide $V_{1.1}Sb_{0.9}O_4$ phase was found in the VSb/Al catalyst [12,13]. XRD peaks of this $VSbO_4$-like phase(s) are detected even for VSb/$Mg_{0.1}$Al. However, these peaks are very weak in the VSb/$Mg_{0.3}$Al and disappear in the VSb/$Mg_{0.5}$Al catalyst. This trend implies the interaction between supported vanadium oxide and MgO-component of the Mg_nAl supports.

H_2-TPR profiles recorded for the VSb/Al and VSb/$Mg_{0.1}$Al catalysts (Fig. 3, curves (a) and (b)) are very similar to each other both in the positions of reduction peaks and H_2-consumption. Broad reduction peak within the range of 350–650 °C (T_{max} at ~550 °C) in the H_2-TPR patterns of these samples displayed high reducibility of their vanadium species under moderate temperatures. In the VSb/$Mg_{0.3}$Al and VSb/$Mg_{0.5}$Al systems (Fig. 3, curves (c) and (d)), broad reduction peak at low temperature disappears partly and the resulting reduction peaks become sharper and shift to higher temperatures. This shift indicates that reducibility of the vanadium species of the V–Sb–O on the Mg-rich supports is reduced.

Fig. 4 shows UV–vis DR spectra recorded for the VSb/Al and VSb/Mg_nAl catalysts after pretreatments, under vacuum at 300 °C and in O_2 flow at 600 °C. For all catalysts, low-energy charge-transfer (LCT) bands originating from the charge transfer between vanadium and oxygen were observed in the 200–500 nm region which is characteristic for V^{5+} [21–23]. The contribution from d–d transition of V^{4+} (d^1) that gives a broad band in the 550–800 nm region [23] is observed only for the VSb/Al catalyst pretreated under vacuum (Fig. 4a). The bands in the 200–500 nm region are almost identical for oxidized VSb/Al and VSb/$Mg_{0.1}$Al samples (Fig. 4b), but the blue-shift of LCT bands toward the lower wavelengths is observed with the further increase of MgO-content indicating a decrease in the degree of vanadium condensation in the VSb/$Mg_{0.3}$Al and VSb/$Mg_{0.5}$Al catalysts.

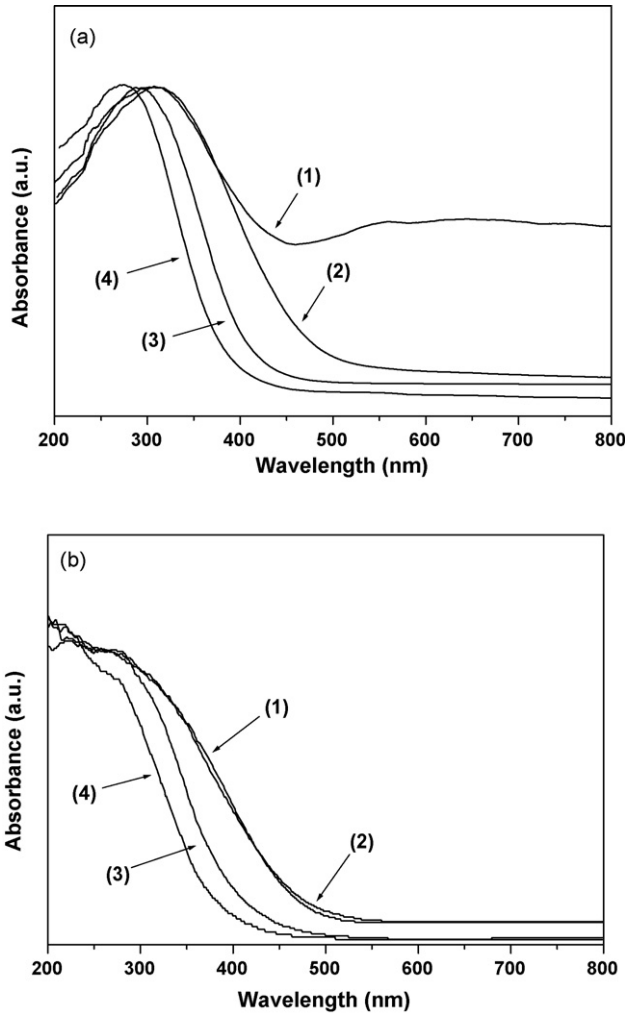

Fig. 4. UV–vis DR spectra of VSb/Al (1) and VSb/Mg_nAl with $n = 0.1$ (2), $n = 0.3$ (3) and $n = 0.5$ (4) pretreated (a) at 300 °C for 1 h under vacuum and (b) at 600 °C for 1 h in O_2-flow.

Fig. 5 presents the NH_3-TPD profiles obtained in order to evaluate the total surface acidity of the VSb/Al and VSb/Mg_nAl catalysts. For all of them, the profiles have similar shapes and the same peaks positions. The amounts of acid sites per catalyst mass unit (Fig. 5) as well as per catalyst-specific surface area unit decrease substantially and steadily with the increase of the Mg-content.

4. Discussion

As shown in Table 1, there is no larger difference of the areal rate of all catalysts studied in this reaction. Therefore, the same active component can be supposed for VSb/Mg_nAl catalysts similar to that of the VSb/Al system whose excellent redox properties determined by dispersed vanadium species and improved by the conjunction with mixed $VSbO_4$-like phase are crucial for the efficient catalysis of the CO_2-EBDH according to a redox Mars-van-Krevelen mechanism [12,13]. The catalysts activity is unambiguously connected with their reducibility (Fig. 3). The VSb/$Mg_{0.1}$Al and VSb/Al catalyst show almost the same initial activities (both in terms of ethylbenzene conversion

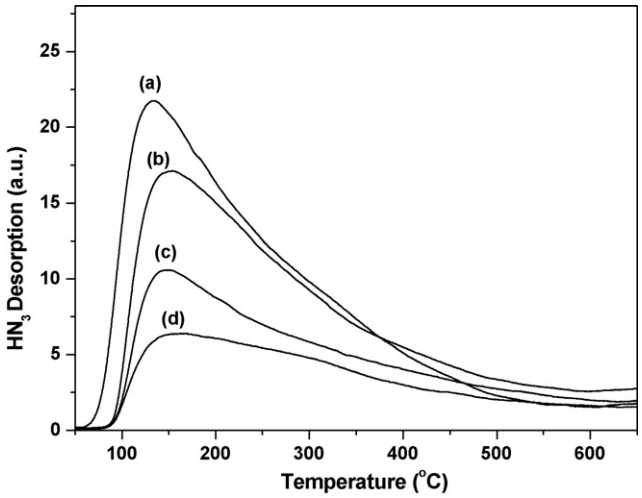

Fig. 5. NH_3-TPD profiles of the (a) VSb/Al and VSb/Mg_nAl catalysts with (b) $n = 0.1$, (c) $n = 0.3$ and (d) $n = 0.5$.

and area-based activity) as well as very similar H_2-TPR profiles. However, both mobility of oxygen and ethylbenzene conversions decrease with further increase of Mg-content in the VSb/$Mg_{0.3}$Al and VSb/$Mg_{0.5}$Al catalysts.

The gradual decrease of the content of active $V_{1.1}Sb_{0.9}O_4$ phase takes place with the increase of MgO-amount (XRD data in Table 1). It can be interpreted as indication in favor of the formation from acid VO_x and basic MgO of Mg–V oxide compound at the expense of V–Sb oxide phase. Magnesium vanadate(s) is, probably, bi-dimensional or sub-surface structure and thus XRD undetectable. The decrease in reducibility of vanadium cations as a result of formation of domains of $Mg_3(VO_4)_2$ in the VO_x/MgO catalysts was reported [24]. Therefore, it could be suggested that some fraction of hard-reducible vanadium species in the VSb/$Mg_{0.3}$Al and VSb/$Mg_{0.5}$Al catalysts might belong to the domains of such magnesium vanadate(s). It is logical to suggest only small contribution of magnesium vanadate(s) domains into bi-dimensional surface vanadium network on the surface of $Mg_{0.1}$Al support whereas in the VSb/$Mg_{0.3}$Al and VSb/$Mg_{0.5}$Al systems with large amount of MgO the sub-surface Mg orthovanadate structure might be formed. In the latter, vanadium species, lying below the surface, are inaccessible for the reagents. As a result, lower ethylbenzene conversions were obtained over the VSb/$Mg_{0.3}$Al and VSb/$Mg_{0.5}$Al catalysts compared to the VSb/Al and VSb/$Mg_{0.1}$Al ones at similar specific (per accessible V-atom) activity.

As shown in UV–vis DR spectra for the catalysts after the pretreatment in oxygen-free conditions in vacuum (Fig. 4a), vanadium species in the VSb/Mg_nAl systems is essentially more resistant towards reduction than V-ion in the VSb/Al. It is consistent with the general trend in the catalysts reducibility while the increase of Mg-content.

The oxidized VSb/Al and VSb/$Mg_{0.1}$Al catalysts display practically identical UV–vis DR spectra (Fig. 4b). However, the further increase of MgO-content in the VSb/$Mg_{0.3}$Al and VSb/$Mg_{0.5}$Al samples has caused the shift in the position of charge-transfer bands toward lower wavelengths. According to [17,21,22], such shift suggests an increase in the degree of VO_x dispersion. Previously it was also shown, for the MgO-supported VO_x catalysts, that interaction between V-atoms and magnesia leads to a high dispersion of $[VO_4]^{3-}$-tetrahedra at low coverages with vanadium and to the formation of magnesium orthovanadate when the vanadium content increases [24,25].

Among three VSb/Mg_nAl catalysts studied, substantial changes in reducibility, dimensionality and degree of dispersion of VO_x species as a result of the Mg-modification of the VSb/Al catalyst were observed for the VSb/$Mg_{0.3}$Al and VSb/$Mg_{0.5}$Al systems. These properties of the most efficient VSb/$Mg_{0.1}$Al catalyst are, however, very similar to those of the VSb/Al one. Meanwhile, the suppression of coking observed for all Mg-containing catalysts is due to the decrease of their surface acidity compared to the VSb/Al (NH_3-TPD data in Fig. 5). The larger pore sizes of the VSb/Mg_nAl catalysts than that of the VSb/Al (Table 1) can also enhance their catalytic stability by facilitating the internal diffusion of styrene in a pore and avoiding its oligomerization leading to the formation of coke precursors.

The avoidance of over-reduction of the catalyst active V^{5+}-species during the reaction also could be an important factor of stable catalytic performance. It was reported earlier that coke formation under the oxidative dehydrogenation of *n*-butane occurs faster on reduced V–Mg–O catalyst than on fully oxidized one [21]. Deep vanadium reduction from V^{5+} to V^{3+} in our previously published VO_x/Al_2O_3 catalyst was observed after several hours of the CO_2-EBDH run. This was considered to be one of the reasons of its much higher deactivation rate compared to that over the VSb/Al catalyst that did not contain V^{3+}-species even after longer catalytic run [13]. The VSb/Mg_nAl catalysts of the current work demonstrate increased resistance of V^{5+} against a reduction along with still more suppressed coking.

At the same time, similar to the results for the propane oxidative dehydrogenation over V–Mg–O catalysts [24], it was shown that fixation of vanadium species in a bulk-like Mg–V compound in the VSb/$Mg_{0.3}$Al and VSb/$Mg_{0.5}$Al catalysts excessively decreases the reducibility of vanadium species (Fig. 3) influencing negatively its accessibility for reagents and, as a consequence, the conversions of ethylbenzene. So, to design the catalyst with reduced coke formation but without loss of its activity, it was necessary to find experimentally an optimal amount of MgO.

We have succeeded in the finding of the VSb/$Mg_{0.1}$Al catalyst in which incorporation of MgO results in substantial improvement of catalytic stability has been achieved through the decrease of the surface acidity (Fig. 5) of the catalyst.

5. Conclusion

Introduction of magnesia into alumina support in the VSb/Al catalyst decreases the surface acidity of the catalysts, leading to the more stable activity in the CO_2-EBDH. However, the modification of the support with MgO leads in general to the decrease of specific surface areas of the catalysts, reducibility of active vanadium oxide component and, therefore, to the

decrease of ethylbenzene conversion. The optimal Mg-content in the alumina support (Mg/Al = 0.1), however, allows to avoid the above-mentioned negative factors and to keep both high activity and catalyst stability.

Acknowledgements

This work was supported by the Institutional Research Program of KRICT (KK-0703-E0). DYH acknowledges the Korea Research Foundation Grant (KRF-2006-351-D00009) and VPV thanks the KOFST for the Brain Pool fellowship.

References

[1] F. Cavani, F. Trifirò, Appl. Catal. A 133 (1995) 219.
[2] N. Mimura, I. Takahara, M. Saito, T. Hattori, K. Ohkuma, M. Ando, Catal. Today 55 (1998) 173.
[3] S. Wang, Z.H. Zhu, Energy Fuel 18 (2004) 1126 (a review).
[4] J.S. Yoo, P.S. Lin, S.D. Elfline, Appl. Catal. A 106 (1993) 259.
[5] M. Sugino, H. Shimada, T. Turuda, H. Miura, N. Ikenaga, T. Suzuki, Appl. Catal. A 121 (1995) 125.
[6] Y. Sakurai, T. Suzaki, K. Nakagawa, N. Ikenaga, H. Aota, T. Suzuki, J. Catal. 209 (2002) 16.
[7] T. Badstube, H. Papp, R. Dziembaj, P. Kuśtrowski, Appl. Catal. A 204 (2000) 153.
[8] A. Sun, Z. Qin, S. Chen, J. Wang, J. Mol. Catal. A: Chem. 210 (2004) 189.
[9] G. Carja, R. Nakamura, T. Aida, H. Niiyama, J. Catal. 218 (2003) 104.
[10] Y. Ohishi, T. Kawabata, T. Shishido, K. Takaki, Q. Zhang, Y. Wang, K. Takehira, J. Mol. Catal. A: Chem. 230 (2005) 49.
[11] J.-S. Chang, S.-E. Park, M.-S. Park, Chem. Lett. 26 (1997) 1123.
[12] V.P. Vislovskiy, J.-S. Chang, M.S. Park, S.-E. Park, Catal. Commun. 3 (2002) 227.
[13] M.-S. Park, V.P. Vislovskiy, J.-S. Chang, Y.-G. Shul, J.S. Yoo, S.-E. Park, Catal. Today 87 (2003) 205.
[14] D.-Y. Hong, J.-S. Chang, V.P. Vislovskiy, S.-E. Park, Y.-H. Park, J.S. Yoo, Chem. Lett. 35 (2006) 28.
[15] J.-S. Chang, D.-Y. Hong, V.P. Vislovskiy, S.-E. Park, Catal. Surv. Asia 11 (2007) 59.
[16] B. Grzybowska, J. Słoczyński, R. Grabowski, K. Wcisło, A. Kozłowska, J. Stoch, J. Zieliński, J. Catal. 178 (1998) 687.
[17] O.R. Evans, A. Bell, T.D. Tilley, J. Catal. 226 (2004) 292.
[18] M. Machli, E. Heracleous, A.A. Lemonidou, Appl. Catal. A 236 (2002) 23.
[19] J.A. Lercher, React. Kinet. Catal. Lett. 20 (1982) 409.
[20] M.L. Pinto, J. Pires, A.P. Carvalho, M.B. de Carvalho, J. Phys. Chem. B. 110 (2006) 250.
[21] C. Tellez, M. Abon, J.A. Dalmon, C. Mirodatos, J. Santamaria, J. Catal. 195 (2000) 113.
[22] E.V. Kondratenko, M. Baerns, Appl. Catal. A 222 (2001) 133.
[23] M.A. Centeno, P. Malet, I. Carrizosa, J.A. Odriozola, J. Phys. Chem. B 104 (2000) 3310.
[24] C. Pak, A.T. Bell, T.D. Tilley, J. Catal. 206 (2002) 49.
[25] T. Blasco, J.M. López Nieto, Colloid Surf. A: Physicohem. Eng. Aspects 115 (1996) 187.